



Master Science, Mention Physique  
Spécialité Physique Subatomique et Astroparticules

Année universitaire **2023-2024**

**Felix TOUCHTE CODJO**

## **PRÉPARATION DE L'EXPÉRIENCE ALERT À JLAB**

Rapport de stage de Master  
sous la direction de Raphaël Dupré

01 mars 2024 au 15 août 2024



**FTC**

## Acknowledgments

I would like to thank my supervisor Raphaël Dupré, for giving me the opportunity to do my internship within his team. You made me feel very welcome. Thanks to you, I met another great people. All the members of the JLab/EIC team of IJCLab were kind. It was very easy to talk with any of them.



## Abstract

The ALERT experiment aims to enhance the understanding of nucleon structure via deep inelastic scattering (DIS) of electrons and to investigate the EMC effect, where the structure of nucleons is modified in different nuclear environments. Key processes such as the deeply virtual Compton scattering (DVCS) and the tagged EMC will be measured on the  ${}^4\text{He}$  nucleus. The Jefferson Lab's Continuous Electron Beam Accelerator Facility (CEBAF), capable of delivering spin-polarized electrons with energies up to 12 GeV, will be used for the experiment. This work proposes a simulation of the ALERT signal for software development purposes.



## Résumé

L'expérience ALERT vise à améliorer la compréhension de la structure des nucléons via la diffusion inélastique profonde des électrons et à étudier l'effet EMC, où la structure des nucléons est modifiée dans différents environnements nucléaires. Des processus clés tels que la diffusion Compton profondément virtuelle et l'EMC étiqueté seront mesurés sur le noyau d'hélium  $^4\text{He}$ . Le Continuous Electron Beam Accelerator Facility (CEBAF) du Jefferson Lab, capable de délivrer des électrons polarisés en spin avec des énergies allant jusqu'à 12 GeV, sera utilisé pour l'expérience. Ce travail propose une simulation du signal d'ALERT à des fins de développement logiciel.



# Contents

<b>Acknowledgments</b>	<b>ii</b>
<b>Abstract</b>	<b>iv</b>
<b>Résumé</b>	<b>vi</b>
<b>Introduction</b>	<b>1</b>
<b>1 Physics motivation</b>	<b>1</b>
1.1 Nucleon structure . . . . .	1
1.1.1 Deep inelastic scattering . . . . .	1
1.1.2 Generalised parton distributions . . . . .	4
1.1.3 EMC effect . . . . .	4
1.2 Proposed measurement . . . . .	6
1.2.1 DVCS . . . . .	6
1.2.2 Tagged EMC . . . . .	6
<b>2 ALERT at Jefferson Lab</b>	<b>8</b>
2.1 CEBAF . . . . .	8
2.2 CLAS12 . . . . .	9
2.3 ALERT . . . . .	10
2.3.1 AHDC . . . . .	10
2.3.2 ATOF . . . . .	11
<b>3 ALERT Simulation</b>	<b>11</b>
3.1 Presentation . . . . .	11
3.2 Digitization . . . . .	15
3.2.1 Event in GEMC . . . . .	15
3.2.2 Drift time calculation . . . . .	16
3.2.3 Signal generation . . . . .	18
<b>Conclusion</b>	<b>20</b>
<b>A Doca calculation</b>	<b>21</b>
<b>B Decoding</b>	<b>22</b>
<b>C Reconstruction</b>	<b>23</b>
<b>Bibliography</b>	<b>25</b>

## List of Figures

1	The Feynman diagram of the deep inelastic scattering at leading order. A virtual photon $\gamma^*$ carries the exchanged four-momentum $q$ . $k$ , $k'$ and $p$ are respectively the four-momenta of the incoming lepton, the outgoing lepton and the target nucleon. . . . .	2
2	Charge distribution of quark inside protons. MMHT2014 NNLO PDFs at $Q^2 = 10 \text{ GeV}^2$ and $Q^2 = 10^4 \text{ GeV}^2$ , with associated 68 % confidence-level uncertainty band. Source [3]. . . . .	3
3	General representation of the GPDs of a nucleon represented by the triple line and noted N. Single lines can represent quarks or anti-quarks probed in the nucleon shown by the triple lines. . . . .	4
4	Illustration of form factors (left), parton distribution functions (center) as an hyperplane of generalized parton distributions (right). Source [6, p. 91] . . . . .	5
5	Ratio of the $\mathcal{F}_2^{IRON}(x, Q^2)$ structure function of iron over the $\mathcal{F}_2^{D_2}(x, Q^2)$ of deuterium. Source [9]. . . . .	5
6	Feynman diagram of a DVCS. . . . .	7
7	The process $A(e, e'(A - 1))X$ within the impulse approximation. . . . .	7
8	Aerial view of the Jefferson Laboratory. The CEBAF continuous electron beam accelerator is represented. The dashed lines indicates the location of the accelerator, and the circle indicates the location of three experimental halls (A,B,C). Source [11, 12]. . . . .	8
9	The CLAS12 spectrometer in Hall-B. The central detectors are contained in the solenoid magnet. The other detectors constituted the forward part of CLAS12. Source [10]. . . . .	9
10	3D view and cutting plan of the layout of the ALERT detector. Source [14]. . . . .	10
11	Wires disposition of the drift chamber of ALERT. A detection cell is highlighted. It is composed a sense wire  surrounded by six field wires  . A potential difference is established between the sense (+) and the field (-) wires to ensure the drift of the electrons created by ionization after the passage a of charged particle. It remains to process the signal collected by the sense wire to determine the position of the particle (see section 3). . . . .	12

12	Picture of the drift chamber of ALERT taken on the premises of IJCLab. On the left, the light of two cell phones is reflected by the sense wires of each super-layers. We clearly see the 20° (from $-10^\circ$ to $+10^\circ$ ) stereo angles between the wires. . . . .	12
13	Picture of the time-of-flight system of ALERT taken on the premises of ANL. The ATOF is fixed at a cart tube. . . . .	13
14	(Left) Drift trajectory of electrons in ALERT for a potential difference of 1.5 kV between the wires in a 5 T magnetic field. The sense wire is at the center and is surrounded by six field wires. (Right) The corresponding isochronous map. Two electrons generated on the same isochronous (closed curve) will reach the sense wire at the same time. Source [14, p. 64]. . . . .	13
15	Mechanism that leads to the signal measured by the drift chamber of ALERT. . . . .	14
16	Signal measured on beam at ALTO by four sense wires during the passage of an $\alpha$ particle of 344 MeV/c. In the first one, no particle passed in AHDC, so the electronics only measured the noise. In the last three, a signal characteristic of an electronic avalanche has been measured due to the passage of a particle in the sensing area. Source [14, p. 94]. . . . .	14
17	Momentum distribution of initial protons generated over ten thousands events in GEMC. . . . .	15
18	(Left) AHDC-like cells with exaggerated concavity for easier visualisation. (Right) A set of steps ( <del>X</del> ) calculated in the same detection cell. The green line represents the trajectory of a particle. . . . .	16
19	Distribution of energy deposited, <b>geant4</b> time, $r$ position and $z$ position of a particular MHit. . . . .	17
20	(Left) Drift time of primary electrons as a function their initial distance to the wire for various gaseous mixtures. The potential difference is still 1.5 kV, the drift chamber being in a 5 T magnetic field. (Right) Estimation of the spatial resolution of the detector as a function of the distance of the step. Source [14]. . . . .	17
21	Deposited energy in each steps as a function of the drift time. . . . .	18
22	Simulation of the AHDC signal. The punctual deposited energies has been changed in energy densities over the time (keV/ns). The time window, the delay and the width parameter of the Landau distributions as been chosen to fit the result of the figure 16. . . . .	19

23	Generated noise at the left and simulated AHDC signal at the right. This figure must be compare to the on-beam measurement of the figure 16. . . . .	20
----	--	----

## List of Tables

1	Specific requirements for the particles to be detected by ALERT. Source [10, 13]. . . . .	10
---	--	----

# Introduction

ALERT is a hadronic physics experiment conducted by teams of IJCLab<sup>1</sup> (France), ANL<sup>2</sup> (USA) and JLab<sup>3</sup> (USA). It bears the name of the brand-new detector ALERT. Combined with the CLAS12 facility of the Jefferson laboratory, the experiment aims to increase our understanding of the nucleon structure. The data taking of the experiment is planed in November 2024.

This report resumes the work done during the starting of my M2 internship at IJCLab. A significant part of my work is bibliography. The section 1 presents the physics motivation the experiment. It reviews the formalism for describing the nucleon structure and presents some measurements proposed during the ALERT experiment. The section 2 describes the experimental setup of the experiment. A description of the components of ALERT is presented. Finally, the section 3 presents simulation work carried out on the ALERT drift chamber.

## 1 Physics motivation

Deep inelastic scattering (DIS) experiments of electrons off nucleons have played a great role in our understanding of the QCD structure of nucleons. It is possible to determine their quark and gluon distributions during inclusive and exclusive processes. These distributions are studied with structure functions such as parton distribution functions (PDFs) and generalized parton distributions (GPDs). More surprising, using nuclear target, it appears that the per-nucleon structure functions depend on the nuclear environment where it has been measured. This modification of nucleon structure in nuclei is known as the "EMC Effect". This section reviews the formalism for the study of nucleon structure and presents some measurements proposed during the ALERT experiment.

### 1.1 Nucleon structure

#### 1.1.1 Deep inelastic scattering

In deep inelastic scattering of a lepton  $e$  ( $k$ ) off a nucleon  $N$  ( $p$ ), only the outgoing lepton  $e'$  ( $k'$ ) is detected, the final state of the nucleon consist of unresolved hadrons "X". The figure 1 shows the Feynman diagram for this process.

---

<sup>1</sup>IJCLab: Irène Joliot-Curie Laboratory

<sup>2</sup>ANL: Argonne National Laboratory

<sup>3</sup>JLab: Jefferson Laboratory

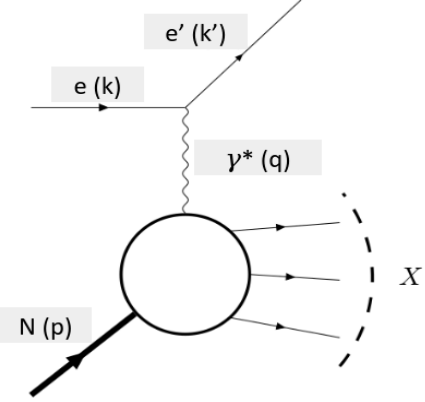


Figure 1: The Feynman diagram of the deep inelastic scattering at leading order. A virtual photon  $\gamma^*$  carries the exchanged four-momentum  $q$ .  $k$ ,  $k'$  and  $p$  are respectively the four-momenta of the incoming lepton, the outgoing lepton and the target nucleon.

The virtuality of the process is defined by  $Q^2 = -q^2 = -(k - k')^2$ . It defines the scale  $\lambda = 1/\sqrt{Q^2}$  at which the incoming nucleon can be probed. The invariant mass of the final state  $X$  is given by  $W^2 = (q + p)^2 \stackrel{lab}{=} M_N^2 + 2M_N\nu - Q^2$ , where  $M_N$  denotes the mass of the target nucleon and  $\nu = \frac{p \cdot q}{M_N} \stackrel{lab}{=} E - E'$  the transferred energy to the lepton via the virtual photon. Two conditions must be satisfied during a DIS [1] :

- $Q^2 > M_N \approx 1 \text{ GeV}^2$ , this allows to interact with partons instead of the whole nucleon.
- $W^2 \gg M_N^2$ , this allows to make sure we break down the nucleon.

The cross section of the DIS can be parameterized by two structure functions  $W_1(\nu, Q^2)$  and  $W_2(\nu, Q^2)$  :

$$\frac{d^2\sigma}{d\Omega dE'} = \frac{\alpha^2 \cos^2\left(\frac{\theta}{2}\right)}{4E^2 \sin^4\left(\frac{\theta}{2}\right)} \left( W_2(\nu, Q^2) + 2W_1(\nu, Q^2) \tan^2\left(\frac{\theta}{2}\right) \right)$$

where  $\alpha$  is the electromagnetic coupling constant,  $\theta$  the scattered angle of the electron and  $d\Omega$  the solid angle of detection. In practice, we use the structure functions  $\mathcal{F}_1(x, Q^2)$  and  $\mathcal{F}_2(x, Q^2)$  defined by :

- $\mathcal{F}_1(x, Q^2) = M_N W_1(\nu, Q^2)$ ;

- $\mathcal{F}_2(x, Q^2) = \nu W_2(\nu, Q^2)$ .

These functions can be expressed in terms of parton distribution functions (PDFs). They are mathematical functions of quark flavour  $q$ , momentum fraction  $x$  and  $Q^2$  :  $f_q(x, Q^2)$ . They represent the probability of finding a quark of flavour  $q$  carrying a longitudinal momentum fraction  $x$ . To define them, let consider<sup>4</sup>  $x_B \equiv \frac{Q^2}{2p \cdot q} \stackrel{\text{lab}}{=} \frac{Q^2}{2M_N\nu}$ , the Bjorken scaling variable. In the Bjorken limit  $\{Q^2, \nu\} \rightarrow \infty$  and at a fixed  $x_B$  value, DIS can be considered as the scattering of a lepton on a free quark.

In other words, the DIS cross section on nucleon can be expressed as the sum of elastic cross section of lepton on the different quark flavors [2] :

$$\left( \frac{d\sigma}{d\Omega dE'} \right)_{N,DIS} = \sum_q \int_0^1 dx e_q^2 f_q(x) \left( \frac{d\sigma}{d\Omega dE'} \right)_{q,ES} \delta(x - x_B)$$

where  $e_q$  is the charge of the quark flavour  $q$ .  $f_q(x, Q^2)$  appears to be normalisation factor. The PDFs of the proton has been determined from fits of world data on DIS. The figure 2 shows the MMHT2014 global fit provided by L. A. Harland-Lang *et al* [3].

It can be shown that  $\mathcal{F}_1(x, Q^2) = \frac{1}{2} \sum_q e_q^2 f_q(x)$  and  $\mathcal{F}_2(x, Q^2) = x \sum_q e_q^2 f_q(x)$ . The identity  $\mathcal{F}_2(x, Q^2) = 2x\mathcal{F}_1(x, Q^2)$  is the Callan-Gross relation.

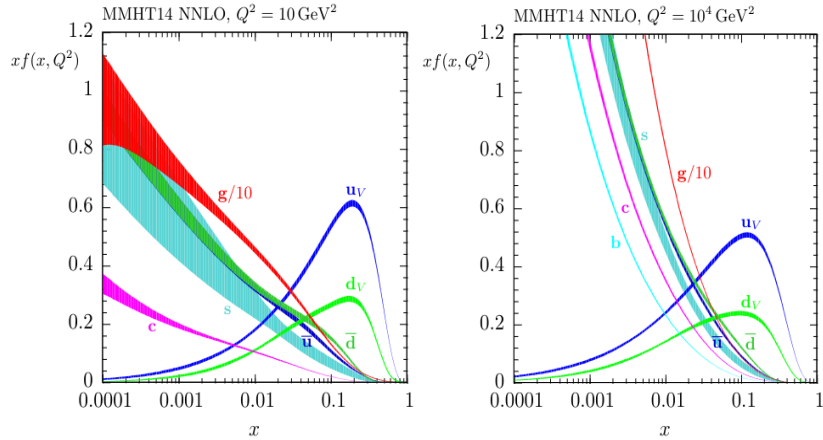


Figure 2: Charge distribution of quarks inside protons. MMHT2014 NNLO PDFs at  $Q^2 = 10 \text{ GeV}^2$  and  $Q^2 = 10^4 \text{ GeV}^2$ , with associated 68 % confidence-level uncertainty band. Source [3].

---

<sup>4</sup>In the lab frame, we consider the target nucleon to be at rest.

### 1.1.2 Generalised parton distributions

We access GPDs in deep scatterings off nucleon where a lepton can interact with a single quark without destroying the nucleon (figure 3). They are real structure functions  $F^q(x, \xi, t)$  of variables  $x$ ,  $\xi$ ,  $\Delta$ . These parameters are defined such that  $x + \xi$  and  $x - \xi$  are the incoming and outgoing quark momenta respectively and  $t = \Delta^2$  is the squared transferred four-momentum [4]. GPDs are a new formalism that starts where perturbative QCD (pQCD) can no longer be applied [5]. These functions encode the correlation between the charge distribution of quarks in the transverse plane and the longitudinal distribution of their momenta (figure 4).

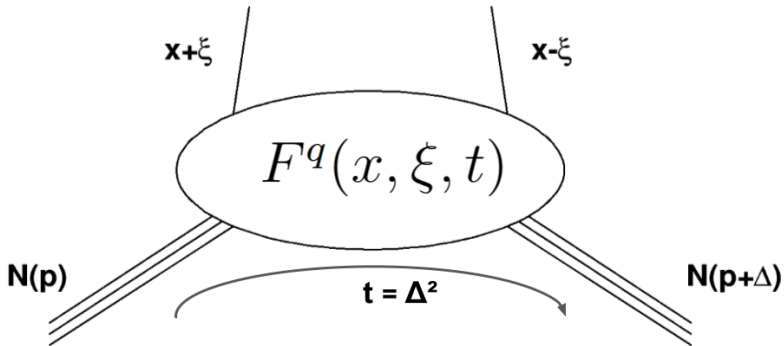


Figure 3: General representation of the GPDs of a nucleon represented by the triple line and noted  $N$ . Single lines can represent quarks or anti-quarks probed in the nucleon shown by the triple lines.

### 1.1.3 EMC effect

The binding energy of nucleons inside nuclei is of the order of few MeV while the mass of nucleons is about 1 GeV. So one could expect that the parton distribution of bound nucleons inside a nucleus should be identical to the parton distribution of a collection of the same number of free nucleons. In this sense, DIS experiments which are sensitive to the partonic structure of the nucleon would give the same result for all nuclei [7]. Instead, the European Muon Collaboration (EMC) found that the per-nucleon ( $e, e'$ ) cross section ratio of iron to deuterium is not unity [8]. The figure 5 is an image of the EMC data as it appeared in the November 1982 issue CERN Courier.

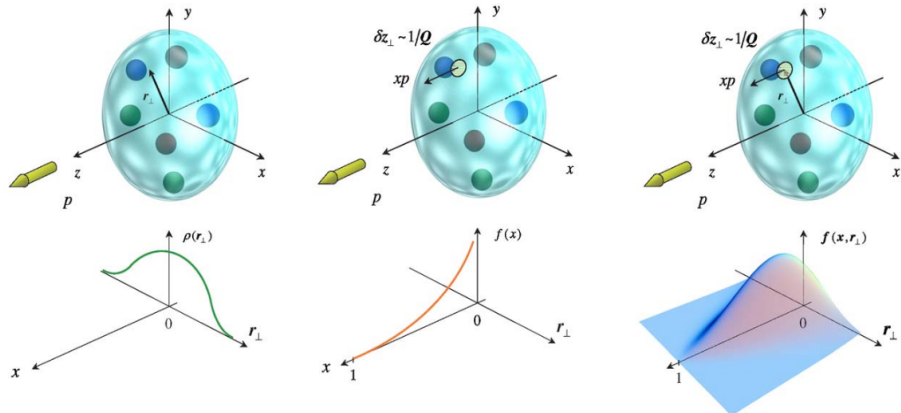


Figure 4: Illustration of form factors (left), parton distribution functions (center) as an hyperplane of generalized parton distributions (right). Source [6, p. 91]

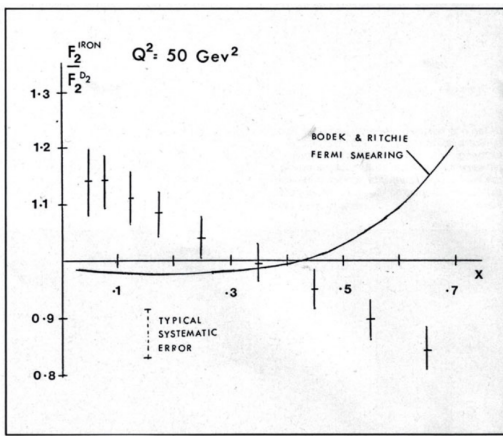


Figure 5: Ratio of the  $F_2^{\text{IRON}}(x, Q^2)$  structure function of iron over the  $F_2^{\text{D}_2}(x, Q^2)$  of deuterium. Source [9].

## 1.2 Proposed measurement

The scientific program of the ALERT experiment is very wide. Among the various processes that will be measured are the DVCS and the Tagged EMC of the  ${}^4\text{He}$  nucleus.

### 1.2.1 DVCS

The Deeply Virtual Compton Scattering (DVCS) is an exclusive process in which a single real photon is produced in the final states of an electron scattering off a nucleus (figure 6). DVCS processes are the simplest road to access GPDs because it limits the possibilities of final state interactions (FSIs). For a spin  $s$  target, the number of chiral-even GPDs is equal to  $(2s + 1)^2$  [10]. So a spin-0 nuclear target as the  ${}^4\text{He}$  has only one chiral-even GPD noted  $H_A$  :  $H_A(x, \xi, t)$ . The process is made in such way that, experimentally, we only have access to the associated Compton form factors (CFF). They are integrated value of GPD over the parameters  $x$ .

If  $F^q(x, \xi, t)$  is a GPD, the corresponding CFF,  $\mathcal{F}(\xi, t)$ , is defined by its real and imaginary part [4]

$$\begin{aligned}\mathcal{R}e(\mathcal{F}(\xi, t)) &= \sum_q e_q^2 \mathcal{P} \int_{-1}^1 dx F^q(x, \xi, t) \left[ \frac{1}{x - \xi} \mp \frac{1}{x + \xi} \right], \\ \mathcal{I}m(\mathcal{F}(\xi, t)) &= -\pi \sum_q e_q^2 [F^q(\xi, \xi, t) \mp F^q(-\xi, \xi, t)].\end{aligned}$$

The ALERT experiment will focus on the measurement of the beam spin asymmetry (BSA) which can be expressed, for the case of a spin-0 target, by:

$$A_{LU}(\phi) = \frac{\alpha_0(\phi) \mathcal{I}m(\mathcal{H}_A)}{\alpha_1(\phi) + \alpha_2(\phi) \mathcal{R}e(\mathcal{H}_A) + \alpha_3(\phi) (\mathcal{R}e(\mathcal{H}_A)^2 + \mathcal{I}m(\mathcal{H}_A)^2)}$$

where  $\phi$  is the angle in the transverse plane and  $\alpha_i(\phi)_i$  factors are  $\phi$ -dependent kinematical terms. So, it remains to fit the BSA as a function of  $\phi$  to resolve  $\mathcal{R}e(\mathcal{H}_A)$  and  $\mathcal{I}m(\mathcal{H}_A)$ .

### 1.2.2 Tagged EMC

The tagged EMC measurement is based on the spectator mechanism (also called plane wave impulse approximation (PWIA)). This is a process where a single virtual photon is absorbed by a quark inside a nucleon and is followed by the recoil of the spectator nucleus  $A - 1$  without any final state interaction (figure 7). Cross section ratios will be measured and studied as function of the kinematic variables of the recoil nucleus detected by ALERT.

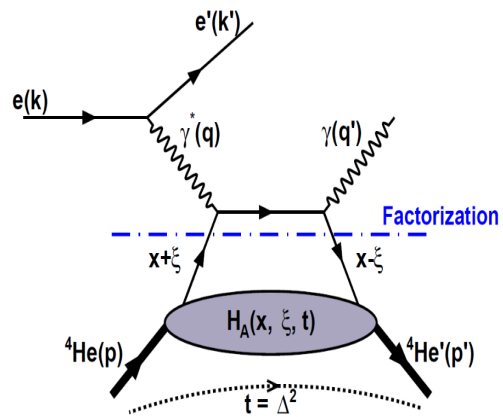


Figure 6: Feynman diagram of a DVCS.

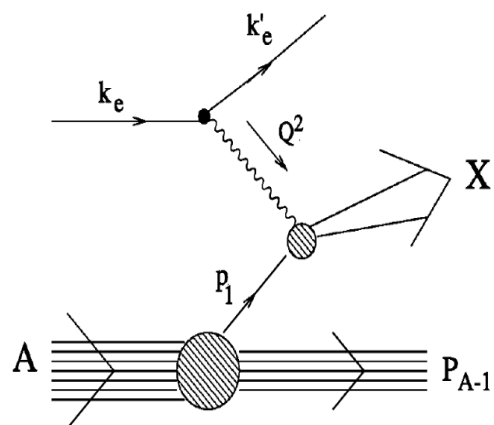


Figure 7: The process  $A(e, e'(A - 1))X$  within the impulse approximation.

## 2 ALERT at Jefferson Lab

The data taking of the ALERT experiment is planned in November 2024. It will take place at the Thomas Jefferson National Accelerator Facility (Jefferson Lab or JLab). Jefferson Lab is a U.S. Department of Energy Office of Science national laboratory. It has been founded in 1984 and is located in Newport News, Virginia, USA. This section present the experimental setup of the experiment with a focus on a (new) low energy recoil tagger (ALERT).

### 2.1 CEBAF

The JLab's research program stands on its Continuous Electron Beam Accelerator Facility (CEBAF) which can deliver spin polarized electrons whose energy can reach 12 GeV. The accelerator is composed of two linear accelerators (linacs) based on superconducting radio frequency technology, connected by two recirculating arcs and arranged in race-track configuration (figure 8). Electrons are generated in a gun and pre-accelerated in the injector before entering the first linac. The system is able to redirect the accelerated electron beam to one of the four experimental halls each time it passes through one linac. It needs to do five turns to reach 11 GeV in Hall-A, Hall-B or Hall-C and one more a half turn to reach 12 GeV in Hall-D. Each hall is dedicated to a specific program of physics. The ALERT detector will be integrated in the spectrometer CLAS12 of the Hall-B.

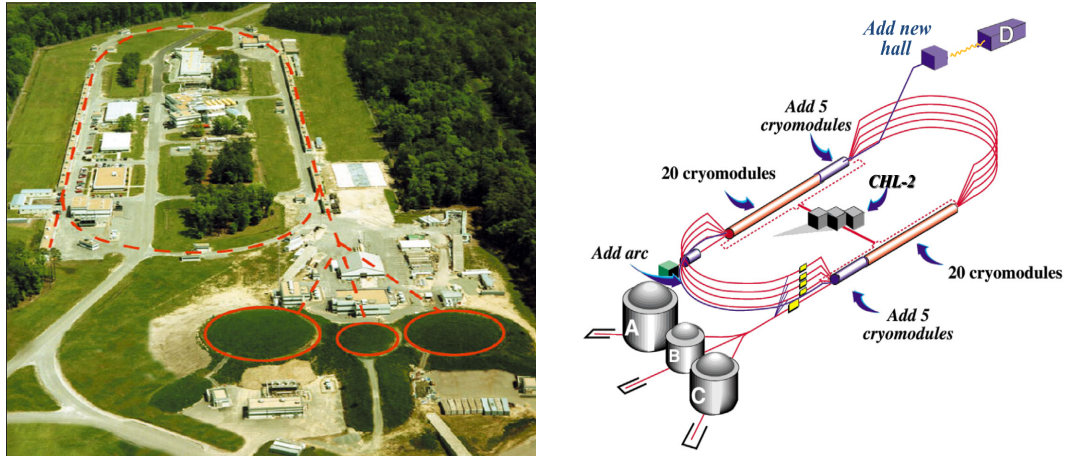


Figure 8: Aerial view of the Jefferson Laboratory. The CEBAF continuous electron beam accelerator is represented. The dashed lines indicates the location of the accelerator, and the circle indicates the location of three experimental halls (A,B,C). Source [11, 12].

## 2.2 CLAS12

CLAS12 stands for CEBAF Large Acceptance Spectrometer for operation at 12 GeV. It consists of a set of sub-detectors aligned along the beam line in the Hall-B. These detectors are divided into two categories: forward and central detectors. Central detectors are immersed in a strong solenoid magnetic field of 5 T while forward detectors are placed in or just after a torus magnet [12]. They are typically drift chambers (DCs), Cherenkov counter (LTCC, HTCC), time-of-flight systems (FTOF, CTOF), electromagnetic calorimeters (ECAL), silicon vertex tracker (SVT) and barrel micromegas tracker (BMT).

The forward part of CLAS12 ensures the detection of particles with  $\theta$  angle<sup>5</sup> ranging from 0° to 35° while the central part ensures the detection of particles with  $\theta$  angle ranging from 35° to 125°. The figure 9 shows all the sub-detectors of CLAS12.

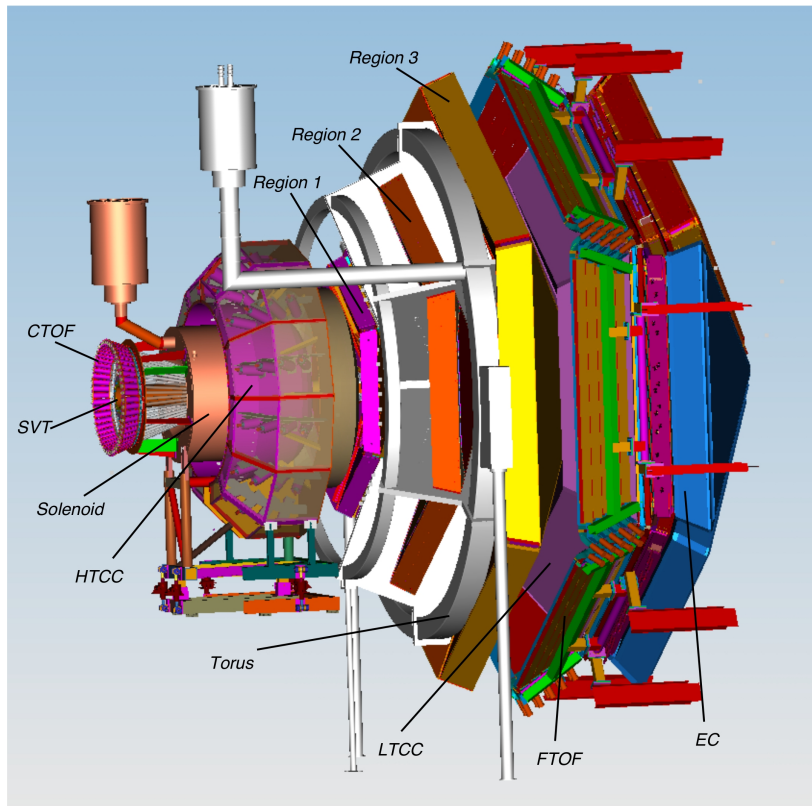


Figure 9: The CLAS12 spectrometer in Hall-B. The central detectors are contained in the solenoid magnet. The other detectors constituted the forward part of CLAS12. Source [10].

---

<sup>5</sup>Angles are given in spherical coordinates.

## 2.3 ALERT

The ALERT detector is composed of an hyperbolic drift chamber (AHDC) and a time-of-flight (ATOF) system. The figure 10 shows the schematic layout of the ALERT detector. It will replace the Silicon Vertex Tracker (SVT) and the Barrel Micromegas (BMT) in the central part of CLAS12 (see figure 9). The table 1 summarizes the types, the momentum ranges and the angular distributions of the particles to be detected with ALERT during each proposed measurements.

Measurement	Particles detected	$p$ range	$\theta$ range
Nuclear GPDs	$^4\text{He}$	$230 < p < 400 \text{ MeV}$	$\pi/4 < \theta < \pi/2 \text{ rad}$
Tageed EMC	$p, ^3\text{H}, ^3\text{He}$	As low as possible	As close to $\pi$ as possible
Tagged DVCS	$p, ^3\text{H}, ^3\text{He}$	As low as possible	As close to $\pi$ as possible

Table 1: Specific requirements for the particles to be detected by ALERT.  
Source [10, 13].

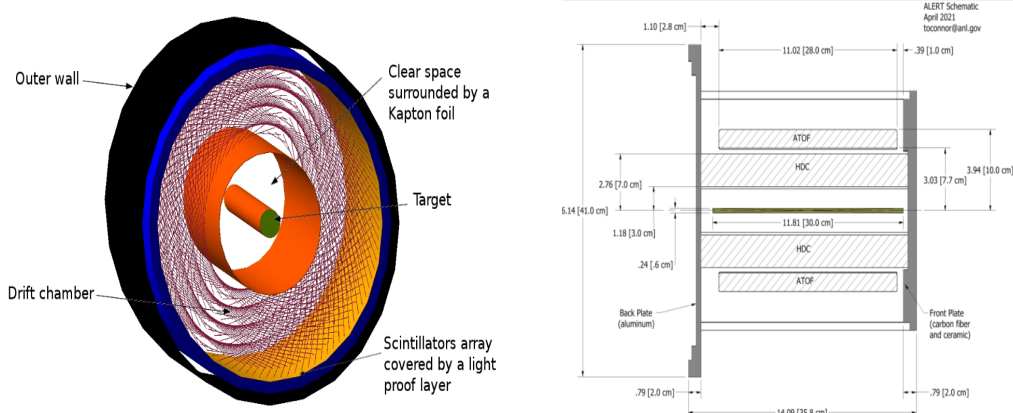


Figure 10: 3D view and cutting plan of the layout of the ALERT detector.  
Source [14].

### 2.3.1 AHDC

The drift chamber of ALERT is a gaseous detector filled with a mixture of He (80 %) and CO<sub>2</sub> (20 %). The tracking of charged particles is ensured by a set of 3026 wires distributed over 21 circular layers centered on the beam

axis [14]. The wires are alternatively oriented either in  $-10^\circ$  or  $+10^\circ$  with respect to the axis of the drift chamber to determine the coordinate along the beam axis ( $z$ ) and gathered in five super-layers of three or five layers. The wires disposition of ALERT is shown in figure 11 and 12.

### 2.3.2 ATOF

The time-of-flight system will surround the AHDC. It is constituted of two layers of scintillators read by silicon photomultipliers (SiPM). The study of the time-of-flight combined with AHDC data will allow to identify the different particles to be detected by ALERT [10].

## 3 ALERT Simulation

The simulation of the ALERT detector is done using GEMC<sup>6</sup>. GEMC is a C++ framework that used Geant4 to simulate the passage of particles through matter. This part describes how to simulate the characteristic signal of the drift chamber of ALERT.

### 3.1 Presentation

When charged particle passes through the volume of the drift chamber, it ionizes the molecules of the gas and creates primary electrons. The electromagnetic field generated by the potential difference between the sense and field wires ensures the drift of these electrons towards the closest sense wire. Without the presence of a magnetic field, it can be show that the electric field is radial and inversely proportional to distance to the sense wire. In presence of an external magnetic field such as the 5 T of the solenoid magnet of CLAS12, the field lines take a more complex form as show in figure 14. In any case, the primary electrons get more and more energy during the drift; their energy becomes enough to ionizes new molecules of the gas and creates secondary electrons. The process {drift, get more energy, ionize} is repeated from the secondary electrons, and so on. That leads to an electronic avalanche. This is the accumulation of charges on the sense wire that generates the signal of the AHDC (figure 15). During the development of the drift chamber, on-beam measurement at ALTO<sup>7</sup> has been done. The typical signal of ALERT is given by the figure 16. The following section describes the process used to retrieved this kind of signal in simulation.

---

<sup>6</sup>GEMC : GEant4 Monte-Carlo

<sup>7</sup>ALTO is research platform located in Orsay, France.

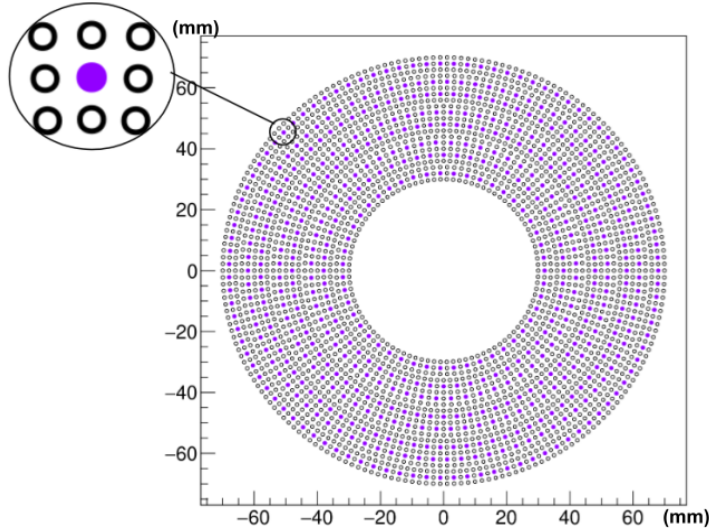


Figure 11: Wires disposition of the drift chamber of ALERT. A detection cell is highlighted. It is composed a sense wire ● surrounded by six field wires ○. A potential difference is established between the sense (+) and the field (−) wires to ensure the drift of the electrons created by ionization after the passage a of charged particle. It remains to process the signal collected by the sense wire to determine the position of the particle (see section 3).

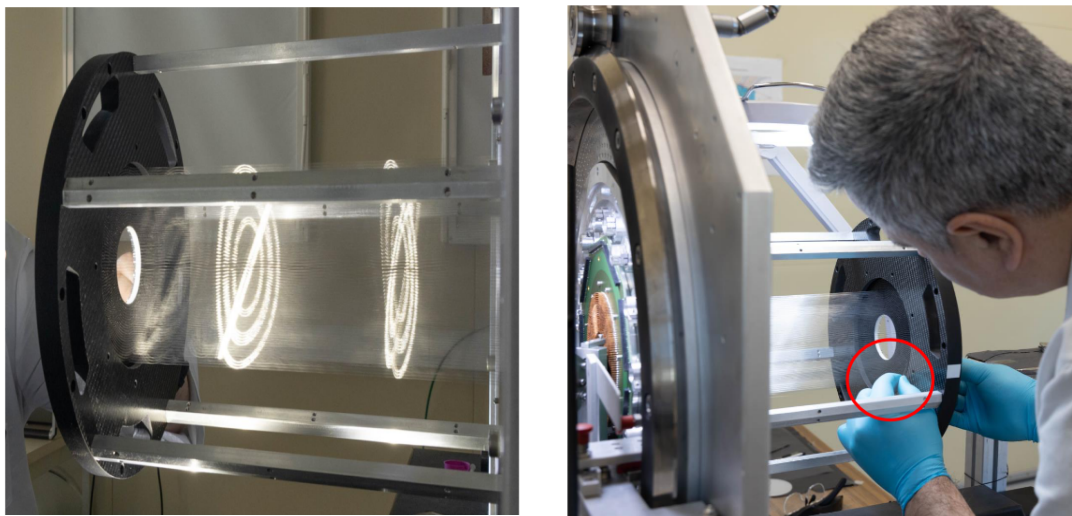


Figure 12: Picture of the drift chamber of ALERT taken on the premises of IJCLab. On the left, the light of two cell phones is reflected by the sense wires of each super-layers. We clearly see the  $20^\circ$  (from  $-10^\circ$  to  $+10^\circ$ ) stereo angles between the wires.

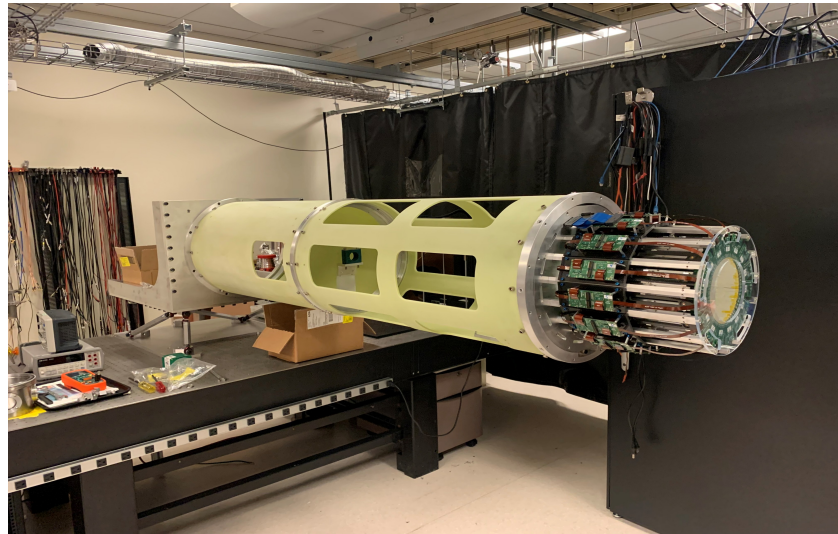


Figure 13: Picture of the time-of-flight system of ALERT taken on the premises of ANL. The ATOF is fixed at a cart tube.

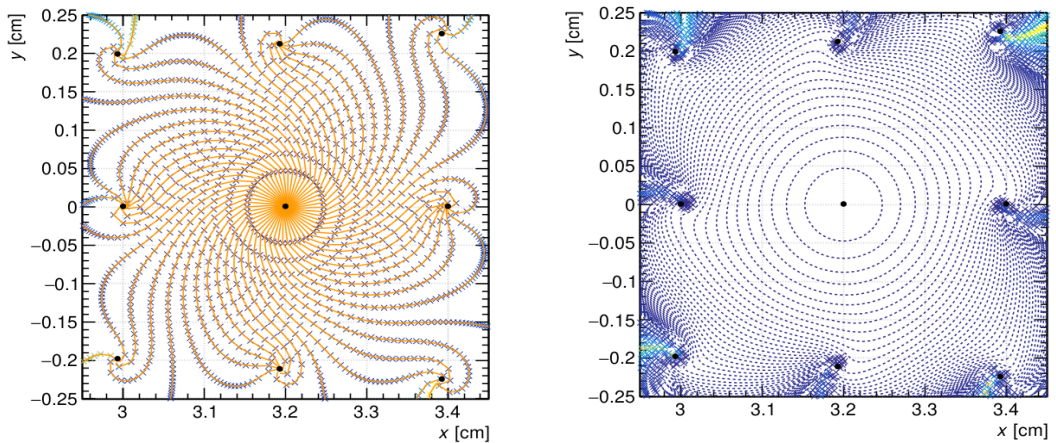


Figure 14: (Left) Drift trajectory of electrons in ALERT for a potential difference of 1.5 kV between the wires in a 5 T magnetic field. The sense wire is at the center and is surrounded by six field wires. (Right) The corresponding isochronous map. Two electrons generated on the same isochronous (closed curve) will reach the sense wire at the same time. Source [14, p. 64].

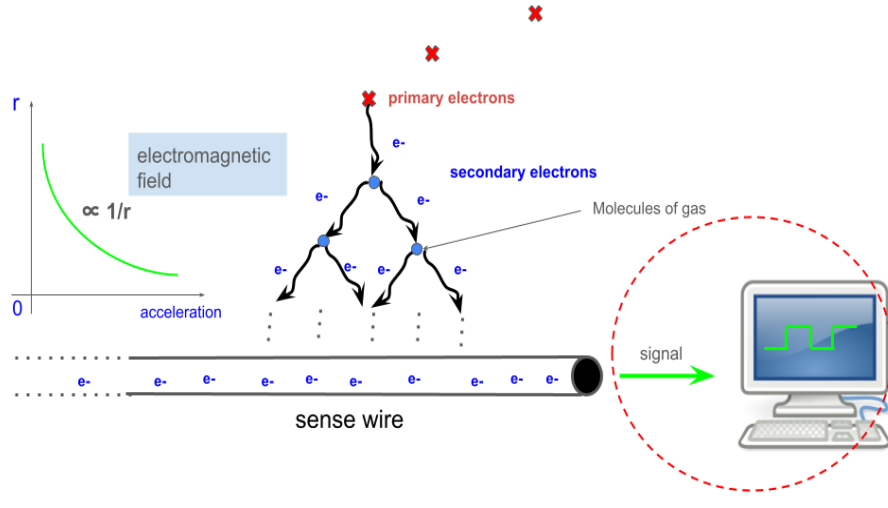


Figure 15: Mechanism that leads to the signal measured by the drift chamber of ALERT.

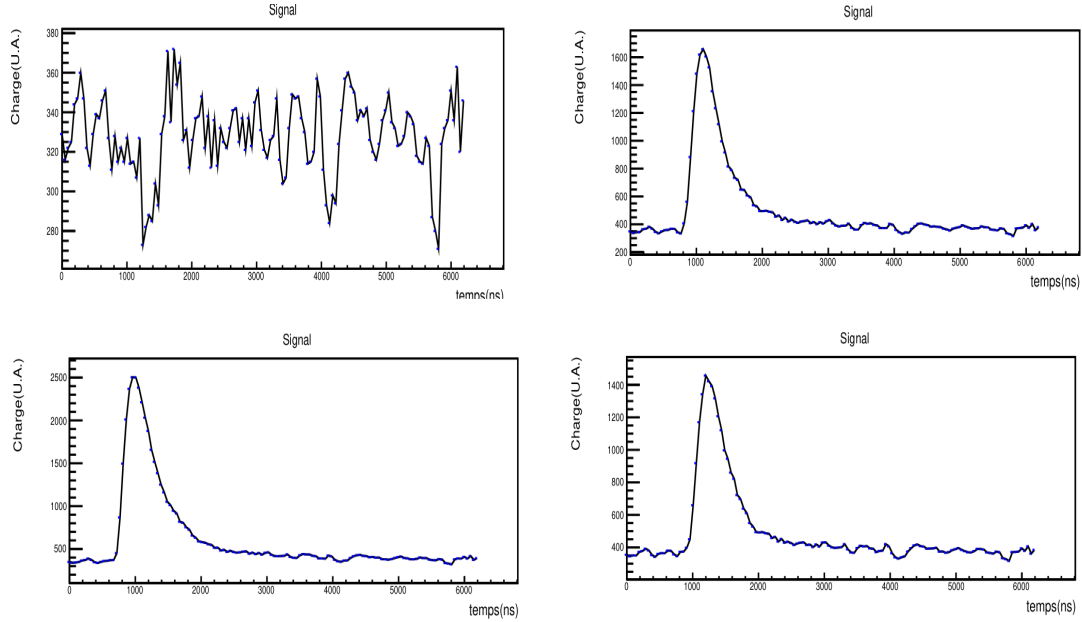


Figure 16: Signal measured on beam at ALTO by four sense wires during the passage of an  $\alpha$  particle of 344 MeV/c. In the first one, no particle passed in AHDC, so the electronics only measured the noise. In the last three, a signal characteristic of an electronic avalanche has been measured due to the passage of a particle in the sensing area. Source [14, p. 94].

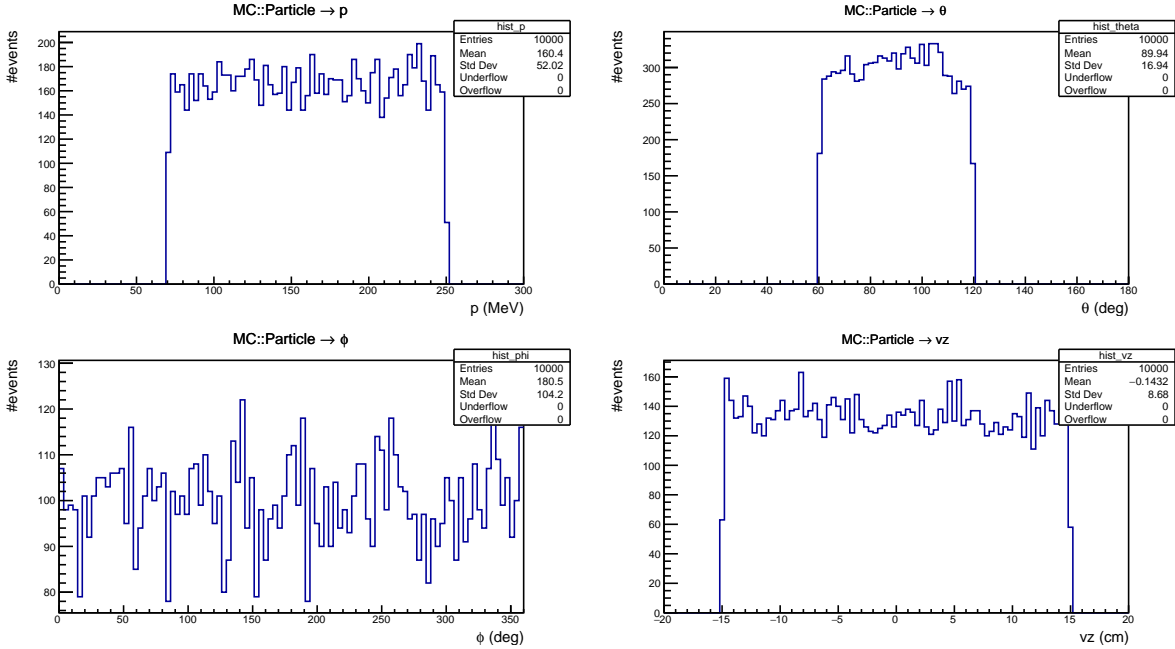


Figure 17: Momentum distribution of initial protons generated over ten thousands events in GEMC.

### 3.2 Digitization

In a very simple manner, one can generate particle of any kind using GEMC. The user only have to specify the initial position and momentum of the particle in a configuration file called `alert.gcard`. The figure 17 shows the momentum distribution of protons generated over ten thousands events.

#### 3.2.1 Event in GEMC

Let consider the propagation of a proton during one event. In GEMC, the track of this particle is segmented in "steps". To simplify, a "step" can be considered as one of the multiple points calculated by Geant4 with the particularity to be a C++ object that contains informations such as :

- the energy deposited in the medium between the last step and the current step ( $\Delta E$ );
- the local and global coordinates of the point ( $x, y, z$ );
- the momentum of the particle at this step of the process ( $p_x, p_y, p_z$ );
- identifiers of the volume of the detector where it has been calculated;

- and so on...

A cell detection of ALERT is encoded by a 3D volume as shown in figure 18. Choosing a sense wire to study corresponds dealing with all the steps calculated (or appearing) in the sensitive zone associated this sense wire. In GEMC, these steps are encoded in a C++ object called **MHit**. The figure 19 shows the distributions of deposited energy, Geant4 time,  $r$  position and  $z$  position that we can find in a particular **MHit**.

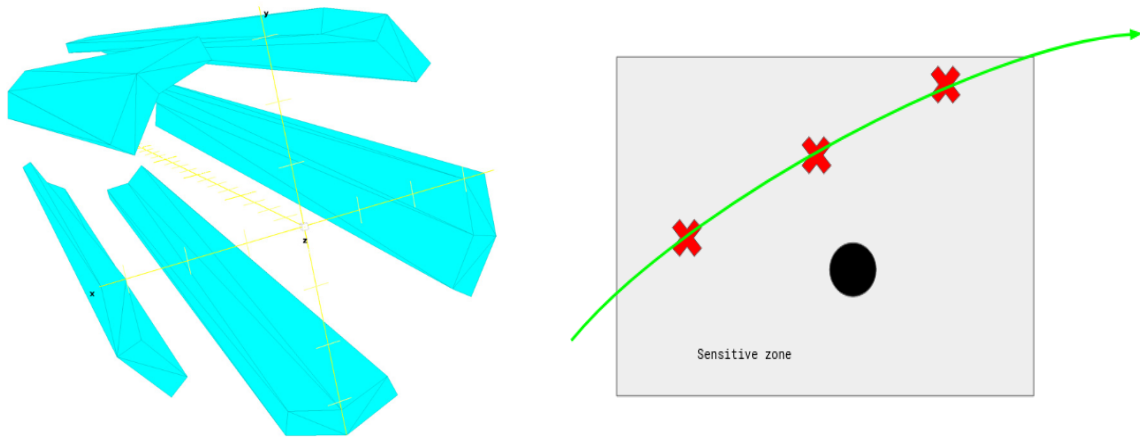


Figure 18: (Left) AHDC-like cells with exaggerated concavity for easier visualisation. (Right) A set of steps ( $\text{X}$ ) calculated in the same detection cell. The green line represents the trajectory of a particle.

### 3.2.2 Drift time calculation

The Geant4 time appearing in the figure 19 is not relevant for the simulation of the AHDC signal. As a first approximation, seeing the isochronous map of the figure 14, we can extract a direct relationship between the drift time a of primary electron created during a step and its initial distance to the wire. The result of mapping time versus distance is shown in the figure 20 (left). The distance to be used is the *doca* (distance of closest approach), defined as the distance from the step point to the wire and perpendicular to the wire (see appendix A). To simulate the spatial resolution of the detector, we compute a new distance by drawing a random number following the normal distribution  $\mathcal{N}(d_{\text{do}}c_a, \sigma_{d_{\text{do}}c_a})$  where  $\sigma_{d_{\text{do}}c_a}$  is also given in the figure 20 (right). Then we use this distance to compute the drift time. The result of this process is shown in the figure 21.

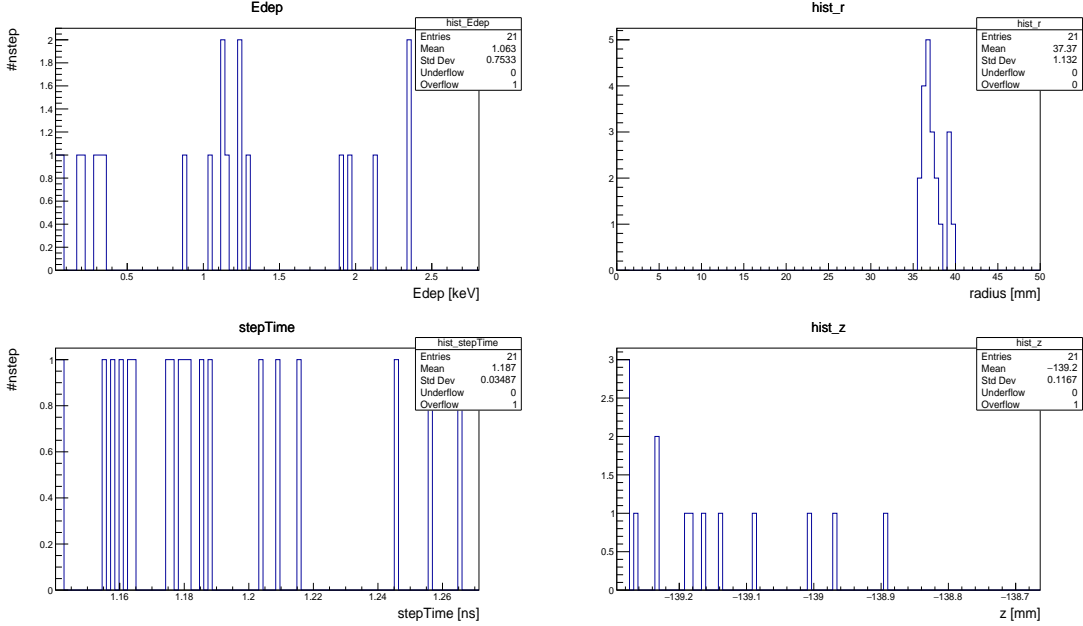


Figure 19: Distribution of energy deposited, geant4 time,  $r$  position and  $z$  position of a particular MHit.

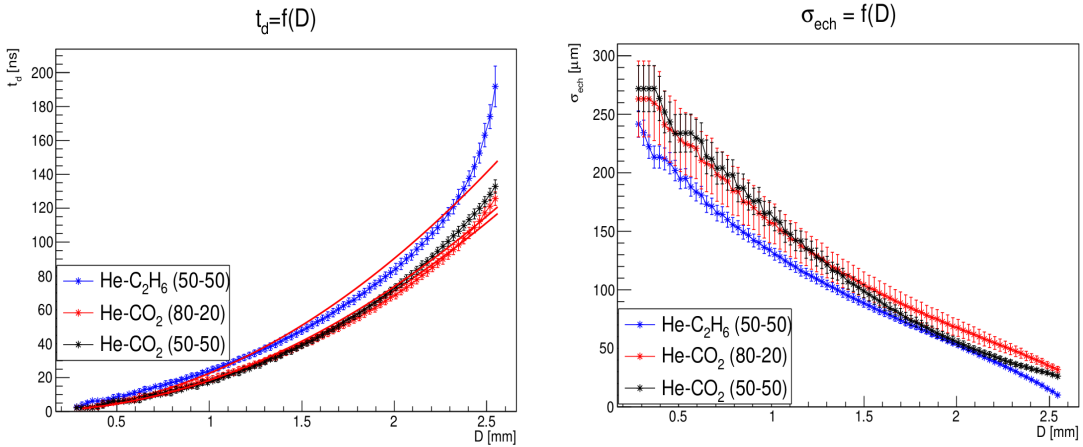


Figure 20: (Left) Drift time of primary electrons as a function their initial distance to the wire for various gaseous mixtures. The potential difference is still 1.5 kV, the drift chamber being in a 5 T magnetic field. (Right) Estimation of the spatial resolution of the detector as a function of the distance of the step. Source [14].

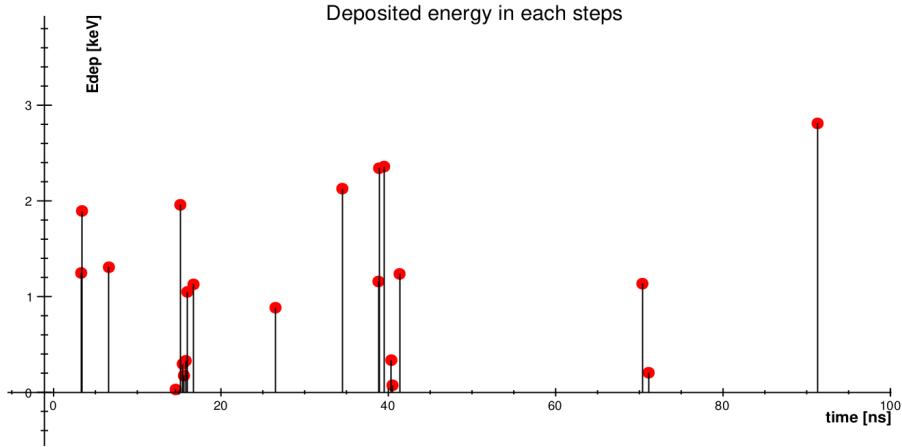


Figure 21: Deposited energy in each steps as a function of the drift time.

### 3.2.3 Signal generation

Punctual distributions are not physical. Indeed on real measurements, we always get a distribution over the time. To simulate that, we spread the deposited energy of each step over the time using a landau distribution. Let be  $\mathcal{L}(x, \sigma, \mu)$  be the normalised Landau distribution where  $\sigma$  is the width parameter and  $\mu$  the location parameter. Fixing  $\sigma$ , each point-like deposited energy  $E_i$  associated at the drift time  $T_i$  is changed by the function of the time  $E_i \cdot \mathcal{L}(t, \sigma, T_i)$ . In that way, the ALERT signal is defined by :

$$\mathcal{S}(t) = \sum_i E_i \cdot \mathcal{L}(t - t_0, \sigma, T_i)$$

where  $t_0$  is the delay. The result is shown in the figure 22 before and after summing all contributions. The last stage of the simulation consists to :

- convert keV/ns to ADC (quantity measured by the electronics of ALERT);
- sample the signal  $\mathcal{S}(t)$ ;
- add noise.

We use a proportionality factor to convert keV/ns to ADC. The sampling is done every 44 ns. The current algorithm to generate the digitized noise signal  $(X_i)_i$  is the following :

- We define a mean value  $x_0$  and standard deviation  $\delta x$ ;
- $X_0$  is a draw of  $\mathcal{N}(x_0, \delta x)$

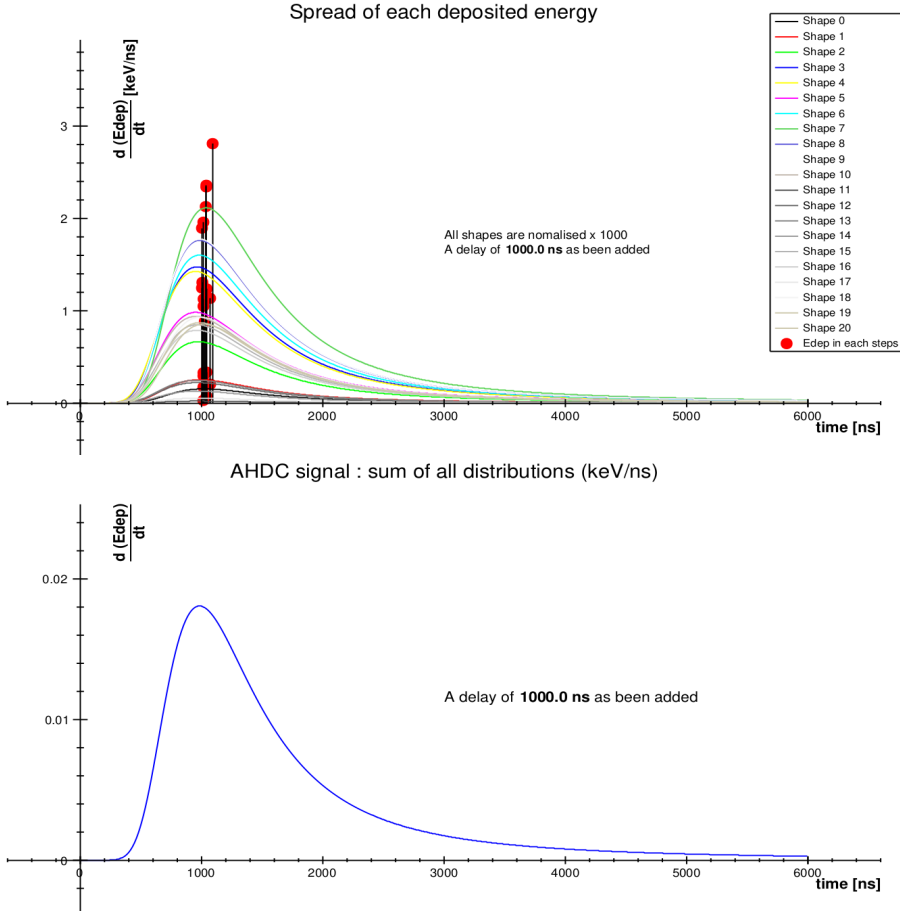


Figure 22: Simulation of the AHDC signal. The punctual deposited energies has been changed in energy densities over the time (keV/ns). The time window, the delay and the width parameter of the Landau distributions as been chosen to fit the result of the figure 16.

- for  $i > 0$ ,  $X_i$  is a draw of  $\mathcal{N}(X_{i-1}, \delta x)$

The final result is given by the figure 23. We can see that we obtain something very similar to the on-beam measurement of the figure 16.

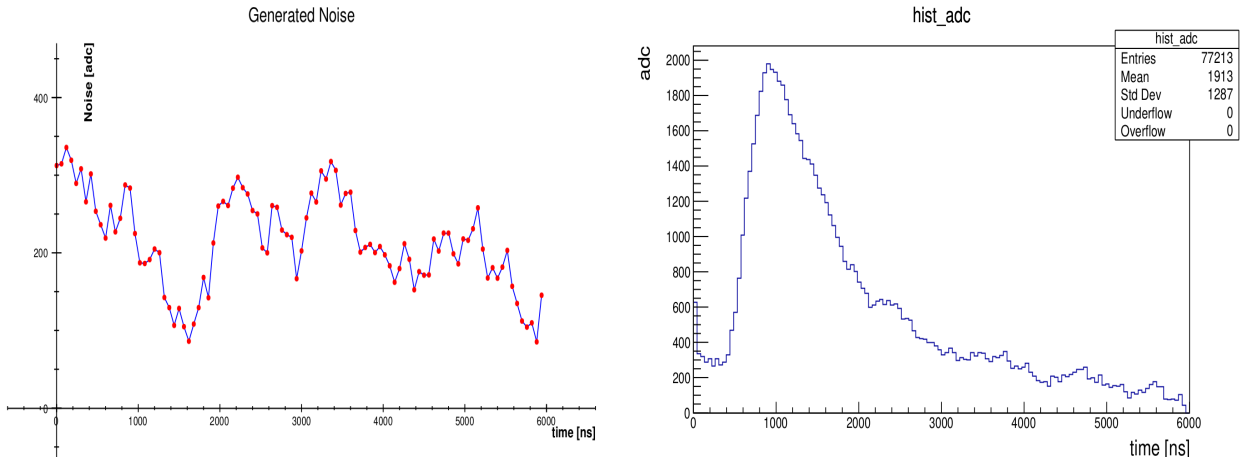
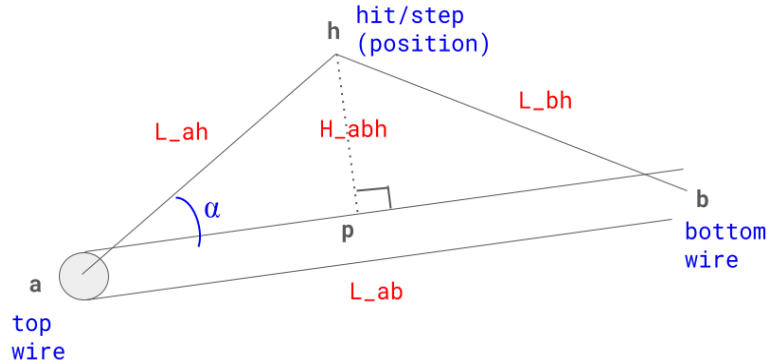


Figure 23: Generated noise at the left and simulated AHDC signal at the right. This figure must be compare to the on-beam measurement of the figure 16.

## Conclusion

The ALERT experiment opens up new ways of investigating the structure of the nucleon. This internship that will continue until the middle of August 2024 is a preparatory work at the experiment planned in November 2024. A big bibliography work has been necessary to understand the expectations of the project. While the construction of the detector is completely done, work on the software part is still in progress. The result obtained on the simulation of the ALERT signal is very promising. The C++ framework developed during the first part of the internship is very consistent. In the remaining time of the project, we plan to study the effect of the noise on the particle detection. Then we will process the simulated signal to extract essential data (see appendix B) for the particle reconstruction (see appendix C).

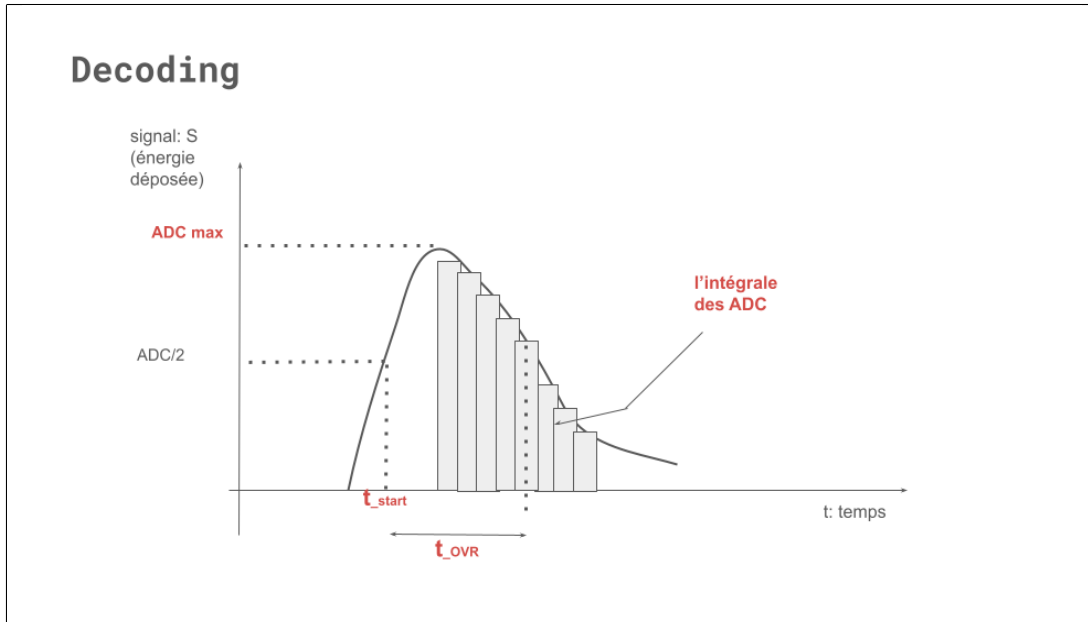
## A Doca calculation



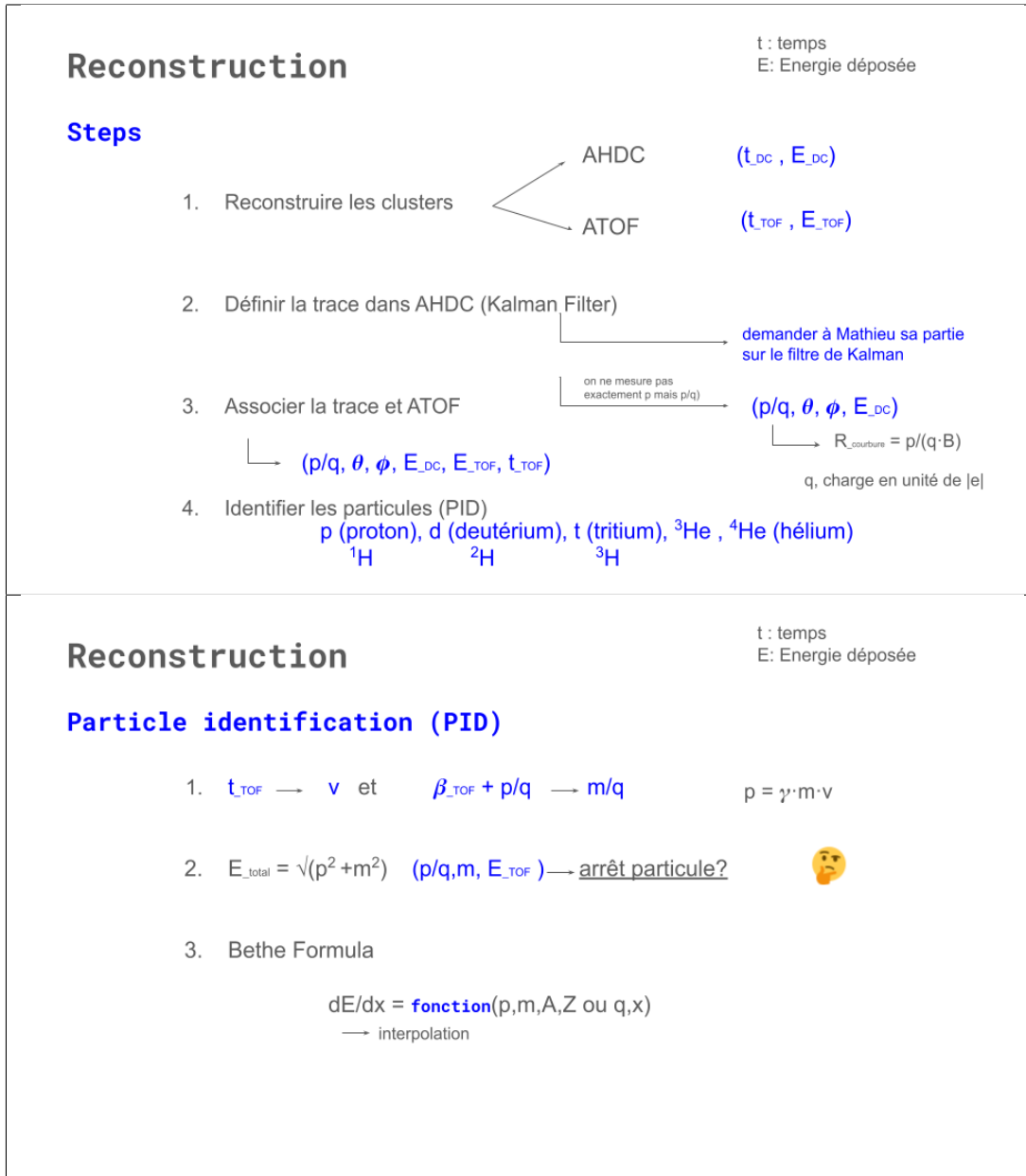
Here the doca is defined by  $H_{abh}$ .

$$\begin{aligned}
 H_{abh} &= HP \\
 &= AH \sin(\alpha) \\
 &= AH \sqrt{1 - \cos^2(\alpha)} \\
 \overrightarrow{HB}^2 &= (\overrightarrow{HA} + \overrightarrow{AB})^2 \\
 &= \overrightarrow{HA}^2 + \overrightarrow{AB}^2 + 2\overrightarrow{HA} \cdot \overrightarrow{AB} \\
 &= \overrightarrow{HA}^2 + \overrightarrow{AB}^2 - 2 \cdot AH \cdot AB \cdot \cos(\alpha) \\
 \cos(\alpha) &= (L_{ah}^2 + L_{ab}^2 - L_{bh}^2) / (2 \cdot L_{ah} \cdot L_{ab})
 \end{aligned} \tag{1}$$

## B Decoding



## C Reconstruction



## References

- [1] Mathieu OUILLON. “Diffusion Compton profondément virtuelle sur le neutron avec l’expérience CLAS12 et le détecteur BONuS12 au laboratoire Jefferson (USA)”. PhD thesis. Particules, Hadrons, Energie et Noyau : Instrumentation, Imagerie, Cosmos et Simulation (PHENIICS), 2024. URL: <https://theses.hal.science/tel-04575566>.
- [2] Mathieu EHRHART. “Nucleon structure studies with CLAS at Jefferson Lab: Deeply virtual Compton Scattering on nitrogen”. PhD thesis. Particules, Hadrons, Energie et Noyau : Instrumentation, Imagerie, Cosmos et Simulation (PHENIICS), 2021. URL: <https://theses.hal.science/tel-03392080/>.
- [3] L. A. Harland-Lang et al. “Parton distributions in the LHC era: MMHT 2014 PDFs”. In: *arXiv* (2014). URL: <https://arxiv.org/abs/1412.3989>.
- [4] The CLAS Collaboration. “Measurement of deeply virtual Compton scattering off Helium-4 with CLAS at Jefferson Lab”. In: *arXiv* (2021). URL: <https://arxiv.org/abs/2102.07419>.
- [5] V. D. Burkert et al. “Colloquium : Gravitational Form Factors of Proton”. In: *arXiv* (2024). URL: <https://arxiv.org/abs/2303.08347>.
- [6] A.V. Belitsky and A.V. Radyushkin. “Unraveling hadron structure with generalized parton distributions”. In: *arXiv* (2005). URL: <https://arxiv.org/abs/hep-ph/0504030>.
- [7] Or Hen et al. “Nucleon-Nucleon Correlations, Short-lived Excitations, and the Quarks Within”. In: *arXiv* (2017). URL: <https://arxiv.org/abs/1611.09748>.
- [8] J.J Aubert et al. “The ratio of the nucleon structure functions F2N for iron and deuterium”. In: *Physics Letters B* (2023). URL: [https://doi.org/10.1016/0370-2693\(83\)90437-9](https://doi.org/10.1016/0370-2693(83)90437-9).
- [9] Douglas Higinbotham et al. “The EMC effect still puzzles after 30 years”. In: *CERN Courier* (2013). URL: <https://cerncourier.com/a/the-emc-effect-still-puzzles-after-30-years/>.
- [10] The CLAS Collaboration. “Partonic Structure of Light Nuclei”. In: *arXiv* (2017). URL: <https://arxiv.org/abs/1708.00888>.
- [11] Douglas Higinbotham. “CEBAF celebrates seven years of physics”. In: *CERN Courier* (2003). URL: <https://cerncourier.com/a/cebaf-celebrates-seven-years-of-physics/>.

- [12] The CLAS Collaboration. “The CLAS12 Spectrometer at Jefferson Laboratory”. In: *Nuclear Instruments and Methods in Physics Research* (2020). URL: <https://doi.org/10.1016/j.nima.2020.163419>.
- [13] The CLAS Collaboration. “Tagged EMC Measurements on Light Nuclei”. In: *arXiv* (2017). URL: <https://arxiv.org/abs/1708.00891>.
- [14] Lucien CAUSSE. “Mise au point d’une chambre à dérive stéréo pour l’expérience ALERT au laboratoire Jefferson”. PhD thesis. Particules, Hadrons, Energie et Noyau : Instrumentation, Imagerie, Cosmos et Simulation (PHENIICS), 2021. URL: <https://theses.hal.science/tel-03613763v1>.